Lab on a Chip

Accepted Manuscript

RSC Publishing

www.rsc.org/loc

Registered Charity Number 207890

Lab on a Chip

RSCPublishing

ARTICLE

Lab-on-Chip Cell-based Biosensor for Label-free Sensing of Water Toxicants

Cite this: DOI: 10.1039/xoxxoooooox

F. Liu,[a] A. N. Nordin,[b] F. Li[c] and I. Voiculescu[a]

Received 23rd September 2013,
Accepted 2nd December 2013

DOI: 10.1039/xoxxoooooox

www.rsc.org/

This paper presents a lab-on-chip biosensor containing an enclosed fluidic cell culturing well seeded with live cells for rapid screening of toxicants in drinking water. The sensor is based on the innovative placement of the working electrodes for electrical cell-substrate impedance sensing (ECIS) technique as the top electrode of a quartz crystal microbalance (QCM) resonator. Cell damage induced by toxic water will cause a decrease in impedance, as well as an increase in the resonant frequency. For water toxicity tests, the biosensor's unique capabilities of performing two complementary measurements simultaneously (impedance and mass-sensing) will increase the accuracy of detection while decreasing the false-positive rate. Bovine aortic endothelial cells (BAECs) were used as toxicity sensing cells. The effects of the toxicants: ammonia, nicotine and aldicarb on cells were monitored with both sensors; the QCM and the ECIS technique. The lab-on-chip was demonstrated to be sensitive to low concentration of toxicants. The responses of BAECs to toxic samples occurred during initial 5 to 20 minutes depending on the type of chemicals and concentrations. Testing the multiparameter biosensor with aldicarb also demonstrated the hypothesis that using two different sensors to monitor the same cell monolayer, provides cross validation and increases the security of detection. For low concentrations of aldicarb, the variations of impedance measurements are insignificant in comparison with the shifts of resonant frequency monitored by the QCM resonator. A highly linear correlation between signal shifts and chemical concentrations was demonstrated for each toxicant.

Introduction

Human access to safe drinking water has become one of the greatest global challenges of this century in the light of increased contamination and scarcity of the world's fresh water supply [1]. The challenge is exacerbated in developing countries where potable water supply is threatened by rapid urbanization, industrialization and excessive farming [2]. To maintain the water quality, clean water supply systems and infrastructure require periodic testing of water samples. Recent advances in miniaturization of mechanical and fluidic devices have inspired a plethora of portable water toxicity sensors based on fluidic biochips [3-5]. Toxicity sensors incorporated in micro total analysis systems (μTAS) are popular for field testing of water samples due to their portability, automation capabilities and sterility [6]. Detection of chemicals in water can be done using antibodies, enzymes, and nucleic acids. Due to the specificity of these devices, array configuration is required to detect a wide range of toxicants [7]. In such applications, label-free sensors using fluorescence probes [8], mass [9] and impedance [10, 11] techniques offer an added advantage and have been used to monitor a wide range of hazardous chemicals in water. To observe the effect of the toxicants on living systems, researchers have incorporated these sensors with live mammalian cells[12-17]. When the cells are exposed to toxicants changes occur in their physiological microenvironment, and they emit biological signals that can be easily converted into electrical signals and monitored. A miniature complete system (biosensor, cell and microfluidics) could then be employed to screen environmental agents or pharmaceutical drugs that are causing perturbations or apoptosis of cells [13, 15]. The advantage of using living cells is that the bioanalytes or toxicants can be monitored without information about the analyte's chemistry. Live cells actively define the transduction mechanism and toxin detection is based solely on physiological cell responses, with cell death being an indicator of a potential threat to human health.

Sensors based on electrical cell-substrate impedance sensing (ECIS) have demonstrated a wide range of applications within biological research, including cytotoxicity studies, drug development, chemokinetic and chemotactic activity of cell and wound healing assays in vitro [18-22]. This method was pioneered by Giaever and Keese, and has been extensively studied for over two decades due to its simple structure, easy operation, and sensitivity to many cell behaviours and properties [6, 7, 23-25]. Mammalian cell-based biosensors using the ECIS technique to

monitor cells viability have been used as toxicity sensors for rapid monitoring of a wide range of toxic industrial chemicals in drinking water [6, 7]. The cells are exposed to toxic water and closely monitored by ECIS technique to assess whether apoptosis (programmed cell death) occurs or not. A reduction in the ECIS impedance measurement corresponds to cell death as an effect of toxicants in the water. The cell-based sensor is not able to evaluate the exact composition of the toxicants in the water but will signal when the water is toxic.

Despite its obvious advantages, several limitations exist in current cell-based toxicity sensors that prevent their use in the field. The large size of the current system and necessity for constant flow of media restricts its field portability and applications as a tool to assess drinking water. Maintenance of viable cells on the chips for long periods of time prior to testing is also problematic. Current toxicity sensors use only a single sensing method that is ECIS, to monitor the cell membrane impedance variations. This limits data collection to information on cell morphological changes and cell movements. Modern technological advancement in lab-on-chip designs and fabrication techniques has created cell maintenance systems that are miniature and highly integrated. Merging a sensor with multiparametric measurement capabilities with microfluidic technology allow researchers to develop a practical bio-fluidic chip, which can be deployed in field stations for rapid analysis. Multiparametric sensing allows cross validation for water toxicity analysis and the microfluidics help maintain long-term cell viability for cytotoxic testing.

In this paper we present a novel label-free sensor used for real-time, rapid and sensitive detection of toxicants in drinking water. The device combines two sensing methods for cross validation and is able to monitor both the cell attachment and viability when exposed to toxicants. The sensors are: (1) a quartz crystal microbalance (QCM) resonator and (2) impedance sensor. Both sensors monitor the same cell monolayer and will signal when the cells are apoptotic due to the presence of toxicants in the water. Two simultaneous, complementary measurements are used to verify the accuracy of our testing results and to minimize false positives.

The QCM is an extremely sensitive mass sensor, capable of measuring mass changes in the nanogram range. This piezoelectric thickness-shear-mode resonator that has been successfully employed for biological sensing applications due to the minimal damping of the acoustic wave in liquid [26-30]. The QCM's sensitive surface can be functionalized with different molecules that respond to different target analytes and have been tested with a wide range of biological applications. The adhesion [27, 29, 31, 32] and visocoelastic[31-33] properties of cell monolayers have been successfully characterized and reported using QCM resonators.

In this research, Bovine aortic endothelial cells are (BAEC) (VEC Technology) were cultured as a monolayer on the sensor. When BAECs attach on this hybrid sensor surface, the acoustic wave detects changes in the biophysical properties of the BAECs such as cell morphology, adhesion, strength by resonant frequency shifts and the insertion loss of the acoustic sensor. The ECIS electrodes on the same sensor give information about nanometer-order dynamics and attachment of the cells. By merging the capabilities of two highly sensitive sensors; acoustic wave and impedance, the same cell culture can be monitored over a period of time, yielding more accurate information compared to measurements using a unique sensor. For rapid studies of water toxicity, the simultaneous response from two different sensors will confirm the security of the drinking water. When the BAECs cultured on this hybrid sensor are exposed to toxicant and are apoptotic the impedance values are minimal since the cells lose their dielectric properties. Apoptotic cells also detach from the QCM electrode and the resonant frequency increases. Water toxicity tests were performed in this work to study the BAECs responsiveness to health-threatening concentrations of ammonia, nicotine, and aldicarb in de-ionized (DI) water.

Computation of Cell Membrane Capacitance and Resistance

The values of the resistance and capacitance of the cell membrane provide important information about the electrophysiological properties of the cell. When the ion channels are blocked, the cell membrane will have higher values of the capacitance. The capacitance and resistance characterizing living cells are significantly different from that of apoptotic cells. Healthy cells adhere more tightly to a surface in comparison to unhealthy or apoptotic cells which results in stronger capacitive coupling between the cells and underlying electrodes. When the cells are apoptotic the cell membranes lose their dielectric properties causing impedance to decrease.

When adherent cells are cultured on the electrodes, cell-related impedance (Z_r) could be considered as a combination of several electrical components. The cells monolayer and the extracellular matrix protein could be represented as a simple electric circuit composed from the resistance and capacitance of different components connected in parallel. In this electric circuit, R_g is considered the resistance across the cell layer including the cell-cell resistance of the gaps between cells, and cells and substrate. C_c is the capacitance of the cell membrane. After the cells attach to the sensing electrode, the total impedance Z_c could be considered as the combination of cell related impedance Z_r and impedance of cell-free system Z_n, as illustrated in Equation (1) [33]

$$Z_r = Z_c - Z_n \quad (1)$$

$$Z_n = R_m + Z_{CPE} = R_m + \frac{1}{Q_0 \omega^n} e^{-\frac{\pi}{2} nj} \quad (2)$$

Z_n could be calculated with equation (2), where Z_{CPE} is constant phase element due to frequency related electrical double layer

capacitance, and R_m is the resistance of the medium. The cell-related impedance Z_r could be calculated with the equation (3) [33]:

$$Z_r = \frac{1}{\frac{1}{R_g} + j\omega C_c} = \frac{R_g}{1+\omega^2 C_c^2 R_g^2} - j\frac{\omega C_c R_g^2}{1+\omega^2 C_c^2 R_g^2} \quad (3)$$

In this research, the resistance and capacitance of the cell layer were extracted by fitting the equivalent circuit model with the experimental measurements of impedance spectroscopy at different time points. The values of the resistance and capacitance of the BAECs are given in Table 1. As illustrated in Table 1 the resistance of the BAECs monolayer increased and the capacitance decreased during the BAECs attachment and spreading phase, which is an indication that the BAECs were strongly attached to the substrate and were in good health.

Table 1: Estimated parameters by fitting the equivalent circuit model into the measurement at different time points.

Time (min)	R_m (Ω)	Q_0 (μF)	n	R_g (Ω)	C_c (nF)
0	89	1.54	0.84	-	-
30				78	15
100				108	10

The cells were cultured on the working and counter ECIS electrodes and electrochemical ECIS measurements were made. Using a design of a small working electrode (less than $10^{-3}cm^2$) and a large counter electrode, the impedance at the working electrode interface dominates the signal and the noise induced by the resistance of electrodes can be ignored. As the area of working electrode is much smaller than that of counter electrode, the contribution of the counter electrode on the measured impedance value is minimal.

Experimental Work

Fabrication of fluidic biochip

The hybrid sensor was fabricated using microfabrication process techniques [34]. The electrodes of the QCM and ECIS were fabricated on an AT-cut commercial quartz substrate with nominal thickness of 100 μm. The QCM top and bottom electrodes have a diameter of 2 mm and were fabricated from thin layers of Cr/Au that were deposited using thermal evaporation on both; the front and back side of the quartz substrate [34]. An array of six identical hybrid biosensors with high-throughput capabilities was fabricated on the quartz substrate, as shown in Figure 1(a). Figure 1(b) is an illustration of the working principle of the hybrid biosensor, which integrates acoustic wave sensing with ECIS technique. An alternating current applied between the top and bottom QCM electrodes generates thickness shear mode acoustic waves that propagate through the quartz substrate. As shown in Figure 1(a), impedance spectroscopy measurements are performed between the top QCM electrode in the center as the ECIS working electrode and the surrounding semicircular counter electrode. The centre-to-centre distance of the adjacent hybrid biosensors is 12 mm.

The sensors are enclosed in a microfluidic polymeric chamber made from polydimethylsiloxane (PDMS) and its top view is shown in Figure 2. Soft photolithography techniques were used to fabricate the culturing chamber using two layers of PDMS[35]. The sterilized cell culture chamber was glued using silicone adhesion on the quartz sensor array, enclosing the working and counter electrodes. This structure was cured at room temperature for 24 hours to reach the optimal bonding.

This culturing chamber incorporates tree-like networks of microfluidic channels (for the media perfusion) leading to the cell culturing chamber and leading away from the chamber (media evacuation). The enclosed cell culture chamber allows automated media delivery to the cells using a portable pump, making it ideal for field tests. The cell culture chamber was designed to meet two requirements for improving long-term cell viability: (1) minimize flow related shear stress effects below the level which can impair cell function and, (2) control cell media flow for equality at all points in the cell culture chamber. Perfusion parallel microchannel barriers shown in Figure 2 were designed on both sides of cell culturing chamber to evenly distribute media over the BAECs [35]. These microchannel barriers were fabricated above the culturing chamber in the top PDMS layer. By locating the media inlets and outlets above the culturing surface the fluid flow path reduces excessive shear stress at the cell surface. In addition to the perfusion inlet and outlet, an extra inlet is provided for cell seeding [35]. The small dimensions of the perfusion channel provides high flow resistance, thus low flow rate control is achieved by appropriate fluidic dimensions for a given head pressure with a concomitant low shear stress applied to the cells during any flow related procedure. With this microfluidic device design, cell media can be automatically perfused into the culturing chamber in laminar fashion. This configuration with microfluidic channel barriers maintains the flowing perfusion media shear stress at low values and contributes to cell longevity. Media could be automatically recirculated over the cells by a portable pump, in order to create the conditions required for testing the sensor in the field.

BAECs Cell Culture on fluidic biochip

Bovine aortic endothelial cells (BAECs) (VEC Technologies, Rensselaer, NY) have been demonstrated in prior research to be sensitive to a range of environmental toxicants and exhibit long-term survival without need for laboratory manipulation[6, 7]. Before the water toxicity tests, the chip was washed with 1x Dulbecco's phosphate buffered saline (DPBS) (Life Technologies, Carlsbad, CA) and sterilized de-ionized (DI) water for three times, followed by exposure to UV light for 10

minutes. 100 µl of extracellular matrix fibronectin (30 µg/ml) was added into the culture chamber to cover the sensor's surface and to improve cell attachment. Prior the experiment, the fibronectin solution was kept at room temperature for 1 hour. BAECs from passage 7 to passage 11 were used for all the water toxicity tests presented in this paper for consistent results. BAECs were subcultured every three or four days. MCDB-131 complete medium (VEC Technonogies, Rensselaer, NY) was used to culture BAECs in T-75 flask. Trypsin and growth media were warmed up to 37ºC prior to passaging cells. The cell passaging process starts with aspiration of media from the culturing flask. Then 5 ml of trypsin was added to wash the cells and quickly aspirated in less than 30 seconds. Subsequently, 3ml of trypsin was added to harvest the cells. This process was observed under a microscope. When more than 90% of cells have detached, the flask was tapped to detach the rest of cells. Next, 12 ml of the media was dispensed into the flask and the bottom of the flask was washed with the mixture for four times to detach the rest of cells that did not come off from the substrate. After that, the cell suspension was transferred from the flask into a 50ml centrifuge tube. The cell suspension was re-suspended for 100 times to separate cell clusters. Cells were counted using a hemacytometer where the concentrations of cell suspension and the total number of cells were both determined. Then 5 ml of cell suspension from the centrifuge tube was dispensed into a new T-75 flask with 10 ml of fresh growth media. The rest of cell suspension was centrifuged at 220 × g for five minutes to pellet the cells followed by aspirating most of the supernatant except for 100-200 µl. To achieve the desired cell concentration (3.4×10^5 cells/ml) for water toxicity detection, the calculated volume of fresh culture media was added into the centrifuge tube to dilute the cell pellet. The solution was re-suspended one hundred times to have a uniform cell distribution. Then 190 µl of cell media was injected into each chip. Cell seeding density of 1×10^5 cells/cm^2 was used for inoculation and this allows the cells to form a confluent layer on the sensor chip in two days.

The sensor chip with inoculated cells was placed in a humidified incubator at 37º C with 5% CO_2. The sensor was connected to a network analyzer and impedance analyzer to obtain simultaneous measurements of resonant frequency and impedance [28]. The resonant frequency and impedance values stabilize within two days indicating that a confluent cell monolayer was formed on the sensor surface. The confluence of cells was confirmed using a microscope. Calcein AM (BD Biosciences, San Jose, CA), a cell-permanent dye that can permeate through cellular membrane into live cells was used to determine cell viability. In live cells the nonfluorescent calcein AM can be converted to a green-fluorescent calcein after the intracellular esterases remove the acetomethoxy group of Calcein AM. To analyze the cell's viability, the stock calcein AM was diluted by Hanks' Balanced Salt Solution (HBSS, Lonza, Walkersville, MD) to 4 µg/mL and 300 uL diluted calcein AM was added into each cell culture well, then the cells were incubated for 30 minutes at 37°C, 5% CO_2 before florescent analysis.

Water Toxicity Testing on Sensor Array

Ammonia, nicotine and aldicarb were used for water toxicity detection. These toxicants were obtained from Fisher Scientific (Fair Lawn, NJ), Alfa Aesar (Ward Hill, MA) and SPEX CertiPrep (Metuchen, NJ) respectively. All the chemicals with different concentrations were prepared in autoclaved deionized (DI) water. DI water is high purity water with mineral ions removed to prevent their effect on cells. The DI water was sterilized for experiments by autoclaving at 121ºC for 30 minutes. Nicotine solutions were used immediately after preparation due to stability issues. All the chemicals were warmed up to 37ºC to avoid the effects of low temperature on the cells prior to testing. When the impedance and resonant frequency values stabilize, indicating that a confluent monolayer of BAECs has formed, media inside the chip was replaced by 190 µl of toxic chemicals at different concentrations. To ensure repeatability and accuracy of results, each concentration of chemicals was tested three times. The toxicity measurements were monitored for one hour. Two control chips were prepared: one with cells cultured in media, the other with cells cultured in DI water. In addition, control samples of cells using testing chemicals and DI water were prepared for visual inspection by time-lapse microscope (Olympus BX51) for comparison.

Ammonia is one of the most highly-produced inorganic chemicals in industry. The toxic and inhibitory effect of ammonia to mammalian cells has been previously reported [36-39]. Ammonia can easily diffuse across cellular membranes and accumulate inside cell bodies and can cause negative effects on cell growth and metabolism by altering intracellular pH, cytoplasmic membrane potential or metabolic pathways [40, 41]. Rapid sensing of ammonia with this multiparametric sensor system is important for field applications. The desired sensitivity range of detection is between Military Exposure Guidelines (MEG) levels of 1.761mM and the Human Lethal Concentration (HLC) of 54.3mM for ammonia. In our experiments, the ammonia tests were performed using ammonia solution with four different concentrations: 5mM, 10mM, 20mM and 40mM.

Nicotine is a primary ingredient of tobacco, which could cause cancer. The carcinogenic potential of nicotine has been identified in animal models and cell culture over the last decade [42]. The detrimental effect of nicotine is caused through a number of different mechanisms such as increase of cholinergic signaling, thereby impeding apoptosis and promoting tumor growth [43]. The toxic effects produced by nicotine to humans, are more harmful than ammonia. Therefore it is important for the multiparametric biosensor to detect nicotine in a rapid and sensitive manner.

Aldicarb is mostly used as an insecticide in agriculture and it is a cholinesterase inhibitor preventing the breakdown of acetylcholine in the synapse [44, 45]. Aldicarb is highly toxic to people and animals. In case of severe poisoning, the victim dies of respiratory failure. Aldicarb is the most toxic insecticide for humans and a number of food poisoning incidents due to residue aldicarb were reported[46]. For field applications, aldicarb is one of the critical chemicals that need to be tested in the water.

Experimental Results and Discussions

Simultaneous measurements of resonant frequency and impedance were performed for one hour to monitor the BAECs responses to different toxicants in the water. Prior the toxic experiments BAECs with concentration of 1×10^5 cells/cm^2 were cultured on the multiparametric device for two days till they formed a uniform monolayer. The resonant frequency shift was obtained by subtracting the resonant frequency of confluent cell monolayer from the resonant frequency values measured when the cells were not present. The normalized impedance shift was obtained by dividing the impedance values obtained after the perfusion of toxicant in the culturing chamber by the initial impedance value of stable cell monolayer. The impedance measurements were performed at a range of frequencies from 40 Hz to 100 kHz. The toxicity results shown for all the experiments were obtained at the optimal frequency of 40 kHz.

Cell responses to ammonia, nicotine and aldicarb are presented in Figure 3. As expected, when exposed to toxicants, the resonant frequency increased and impedance values decreased which indicate morphological changes of cells; the BAECs monolayer is not firmly attached or has detached from the quartz substrate and the cell-cell contact is disrupted by the toxicant.

Figure 3(a) shows the resonant frequency shift corresponding to four different concentrations of ammonia (5mM, 10mM, 20mM and 40mM). The frequency shifts increase linearly with increasing concentration before it starts to saturate at a specific level. The saturation limits or maximum frequency shifts are 1000 Hz, 1200 Hz, 1500 Hz and 2250 Hz, respectively, corresponding to different concentrations of 5mM, 10mM, 20mM and 40mM. At 5mM, the resonant frequency increased at a rate of 21 Hz/min during the first 40 minutes after the toxicant perfusion, followed by a much slower increase rate (7 Hz/min) for the next 20 minutes. At 10 mM of ammonia, the initial resonant frequency increased at a rate of 36 Hz/min for 33 minutes before it becomes stable for the rest of time. At 20 mM, the resonance frequency takes 27 minutes to stabilize at a rate of 56 Hz/min. The highest concentration of 40 mM takes only 18 minutes to stabilize at a rate of 125 Hz/min.
In Figure 3(b), the decrease of impedance values varied depending on different concentrations of ammonia in DI water. Normalized impedance of 0.6, 0.5 and 0.4 were reached at ammonia concentrations of 10mM, 20mM and 40mM, respectively within 20 minutes. The normalized values of the impedance, for 5 mM ammonia constantly decrease in the first hour. No stable impedance values were obtained. Constant and stable impedance values are an indication that all the cells are apoptotic. Continuous diminutions of impedance values at 5 mM were observed for one hour with fast decrease in first 30 minutes followed by slower decrease. During this time interval the impedance did not reach a constant value because some of the BAECs were still alive. For low ammonia concentrations, a time interval longer than one hour is required for the BAECs to get apoptotic. For this experiment two types of control wells were used. The first control well (control 1) contained BAECs with media and the second control well (control 2) contained BAECs cultured in DI water. DI water was used to dilute all the toxicants in these experiments and thus, it is very important to observe the effect of DI water on BAECs' viability. The resonant frequency and impedance maintained constant values for control 1 indicating that the cells were in good health and cultured in a confluent monolayer. Very small variances of both impedimetric and gravimetric measurements were detected between control 1 and control 2. These small variations were due to the combined effects of different osmolarity and pH values corresponding to DI water on the BAECs. The DI water did not affect the BAECs viability for the time interval of the experiment, which was one hour.

For nicotine testing on the fluidic biochip, the BAECs monolayer was exposed to different concentrations of nicotine: 0.6 mM, 1.2 mM, 2.4 mM and 4.8 mM. Simultaneous resonant frequency and impedance measurements were performed to monitor the cells' response to nicotine solution as shown in Figures 3 (c) and (d). The maximum changes of resonant frequency corresponding to nicotine concentrations of 4.8 mM, 2.4 mM, 1.2 mM and 0.6 mM were 2800 Hz, 1800 Hz, 1300 Hz and 1000 Hz, respectively. The resonant frequency shifts become stable after approximately 15 minutes for the three lower concentrations. At the highest nicotine concentration of 4.8 mM, marked increase of the resonant frequency shift occurred during initial 10 minutes followed by a stabilized frequency value. The different changing rates at different concentrations reflect the degree of detrimental effect of nicotine on the BAEC monolayer. These results suggested that the higher increase rate of resonant frequency at higher nicotine concentration indicated severe degradation of physiological properties and integrity of BAECs monolayer.

As illustrated in Figure 3 (d), the largest decrease rate of impedance was produced by 4.8 mM nicotine. In this case, there was a substantial decrease of impedance during the initial 40 minutes after the BAECs were exposed to nicotine. This was followed by a slower decrease of the impedance after 20 minutes reaching the normalized value of 0.2 at the end of the experiment, which lasted 60 minutes. The normalized impedance values for nicotine concentrations of 2.4 mM, 1.2 mM and 0.6 mM were 0.5, 0.8 and 0.9, respectively. At these

three concentrations, the largest changing rate of impedance occurred within the initial 15 minutes. After 15 minutes the impedance continued to decrease at a much slower rate when exposed to 2.4 mM of nicotine. The impedance values at 1.2 mM and 0.6mM nicotine also approached constant magnitudes after 15 minutes.

The last toxicant that was tested with the multiparametric device was aldicarb. The simultaneous measurement results of impedance and resonant frequency are presented in Figures 3 (e) and (f). The BAEC monolayer responses to 0.05 mM, 0.1 mM, 0.2 mM and 0.4 mM aldicarb were monitored for one hour. As illustrated Figure 3 (e), the maximum shifts of resonant frequency at 0.05 mM, 0.1 mM, 0.2 mM and 0.4 mM were 500 Hz, 600 Hz, 800 Hz and 1100 Hz, respectively. At 0.4 mM aldicarb, the sharp increase of resonant frequency shift occurred in first 5 to 10 minutes followed by a small fluctuation at around 1100 Hz. At the other three lower concentrations of aldicarb, the resonant frequency underwent a relatively slow increase for about 30 minutes before becoming stable.

Simultaneous impedimetric measurement is presented in Figure 3(f) where the minimum normalized impedance values corresponding to the stimuli of 0.4 mM, 0.2 mM, 0.1 mM and 0.05 mM aldicarb were 0.58, 0.75, 0.85 and 0.89, respectively. The BAECs monolayer exposed to concentrations of 0.4 mM and 0.2 mM aldicarb, underwent a continuous deterioration in the first 5 to 10 minutes before the impedance values stabilize indicating that most of the BAECs are apoptotic. The relatively low change of impedance values produced by the aldicarb with concentrations of 0.1 mM and 0.05 mM suggested that the detrimental effect of this toxicant on BAECs was less noticeable with the ECIS sensor. The resonant frequency shifts corresponding to low concentration of aldicarb were more evident with noticeable values of 500 Hz and 600 Hz. Testing the multiparameter biosensor with aldicarb demonstrated the hypothesis that two different sensors could provide cross validation and increase the security of detection. In the case when the impedance sensor will not be able to sense very low concentrations of aldicarb, the QCM sensor will be able to signal the presence of this toxicant in the field water.

As mentioned previously, in the impedance spectroscopy technique cells are considered as insulating particles that restrict the current flow through electrolytic media due to the dielectric property of cellular membranes. Impedance measurement can be used to detect the change of gaps between cell-and-cell or cell-and-substrate, and also the integrity of cellular membranes. The simultaneous gravimetric measurement can both monitor the alteration of adhering strength between cells and substrate and also the viscoelastic properties of cell bodies. According to the graphs (Figure 3), the noticeable difference of toxicity measurements between control 1 (cells in media) and control 2 (cells in DI water) suggested that the toxic chemicals (ammonia, nicotine, and aldicarb) at different concentrations affected the integrity of BAECs monolayer and the intercellular junction of BAEC monolayer. The toxic effects of ammonia, nicotine, and aldicarb on BAECs were suggested in general from the decrease of impedance values and increase of resonant frequency values. It was assumed that the BAECs exposed to toxicants underwent morphological changes, which resulted in increasing the distances between the cell monolayer and substrate and augmentation of the intercellular distances, allowing more current to flow through the cells, thus decreasing the impedance values. The toxicants disrupt the cell membrane causing them to lose their dielectric properties leading to the decrease of impedance. For gravimetric measurements, the penetration depth of acoustic waves into the liquid medium is about 147 nm (assuming the density and viscosity of media is the same as that of water). Increasing the distance between cells and substrate results in less mass that can be probed by the gravimetric sensing method, producing an increase in resonant frequency shift.

The morphological changes of BAECs exposed to ammonia, nicotine and aldicarb were also confirmed by visual inspection using a microscope. Figure 4 (a) shows BAECs cultured in a uniform monolayer with seeding density of 1×10^5 cells/cm^2 before the start toxicity tests. Figure 4 (b), (c) and (d) present BAECs at 30 minutes after exposure to 0.1mM aldicarb, 40 mM ammonia and 2.4 mM nicotine. There is a clear difference between the BAECs unexposed to toxicants and cells exposed to toxicants. The BAECs exposed to toxicants become round as an indication that the cell-to-cell junctions and the cell-to-substrate attachment are damaged by the toxicants. It is possible that these changes of cell morphology produced a rearrangement of cellular cytoskeleton, modifying the viscoelastic properties of cells [45, 46]. Research on cells viscosity monitoring using QCM presented in literature have reported the same conclusion when adherent cells are treated with agents affecting the actin and microtubule cytoskeleton [27, 45].

Figures 4 (e and f) show the fluorescence images of BAECs labeled with Calcein AM, before the toxicity experiment and 10 minutes after introducing 20 mM ammonia. The live cells stained with Calcein AM are in green under fluorescent excitation. Before exposure to ammonia (Figure 4(e)), the BAECs are in good health with all the viable cells forming a monolayer and are stained green under the florescent light. Apoptotic cells are not tagged with Calcein AM and are dark under fluorescent light. Figure 4(f) illustrates BAECs 10 minutes after exposure to 20 mM ammonia. At this moment, only a few cells are still viable and the distances between these viable cells are large with the majority of the BAECs being apoptotic. In this situation, the impedance values are low since current can easily flow from the working electrode to counter electrode in the large gaps between cells. The impedance values do not reach zero after one hour since there are still a few viable cells. When all the cells are apoptotic the impedance values reach zero.

The linearity lines of the multiparametric sensor with respect to the three toxicants were graphed as shown in Figure 5. For the experiments with ammonia, nicotine, and aldicarb, the linear regression generated significant values such as: 0.9982, 0.9993 and 0.9942 respectively for gravimetric measurements, and 0.8072, 0.9751 and 0.9989 for impedimetric measurements. When comparing Figures 5(a) and (b), it can be seen that to generate similar changes in resonant frequency shift, ten times more concentration ammonia is required compared to nicotine. This indicates that the BAECs are much more sensitive to nicotine than ammonia. Similarly, when Figures 5(b) and (c) are compared it is observed that a higher concentration of nicotine is required to produce the same level of signal change produced by the toxicant aldicarb. This suggests that aldicarb is the most toxic for the BAECs compared to ammonia and nicotine. From the analysis of response time in Figures 3, although the concentration of nicotine and aldicarb was much lower than ammonia, faster responses of BAECs to nicotine and aldicarb were achieved. It is reasonable to assume that BAECs are more sensitive to nicotine and aldicarb compared to ammonia.

Conclusions

The multiparametric biosensors integrated with miniaturized enclosed polymeric chambers could be used to assess water toxicity. Confluent monolayer BAECs were chosen as sensing cells for water toxicants. Cell monolayers take up to 40 hours to form on this device. When used in the field for water testing, military personnel will receive the device with the BAECs already cultured as a compact monolayer. All the experiments using a sensor based on live cells have to be performed during the cells' lifetime. Having exact information about the BAECs longevity is important, because the biosensor's shelf life is limited by the lifetime of the cells. When BAECs will be used the cells viability has been determined to be approximately 30 days[35]. During this time period the sensor will give reliable information when field water will be screened.

In this research, simultaneous gravimetric and impedimetric measurements were performed for one hour to continuously monitor the BAECs responses to three different chemicals: ammonia, nicotine and aldicarb. The positive shift of resonant frequency and negative shift of impedance values were successfully monitored at different concentrations of chemicals within one hour. The most significant responses of BAECs to toxic samples occurred during initial 5 to 20 minutes depending on the type of chemicals and concentrations. A highly linear correlation between signal shifts and chemical concentrations was obtained for each chemical. Testing the multiparameter biosensor with aldicarb also demonstrated the hypothesis that two different sensors could increase the security of detection. For low concentrations of aldicarb, the variations of impedance measurements are insignificant in comparison with the shifts of resonant frequency monitored by the QCM resonator. This demonstrates that the usage of multiparametric sensor provides cross validation with increased detection abilities compared to the situation when only a single sensing technique is employed.

For field station deployment, the cell-based sensor necessitates a miniaturized cell culture chip that has the capability to maintain automatic long-term cell viability with low cell media consumption. Long-term cell maintenance requires the device to provide suitable physiological conditions for cells, including cell culture media composition, pressure, shear stress, temperature, pH, and chemical and geometrical microenvironment. In the future, this multiparametric biosensor will be enclosed in a portable incubator for long-term cell viability maintenance, that will allow water toxicity detection tests in field operations.

Acknowledgements

This work was supported by the US Army Research Office, grant number: W911NF-10-1-0150, US Army Research Office and MIT-ISN HBCU-MI program, US Army Centre of Environmental Health Research (USACEHR), contract number: W81XWH-11-C-0026 and the Romanian National Authority for Scientific Research, CNDI–UEFISCDI project number PN-II-PT-PCCA-2011-3.2-1682. This work is also supported by Malaysian Science Fund (SF12-019-0048) and Prototype Research Grant (PRGS 12-010-0010). The content of the information does not necessarily reflect the position or the policy of the Government or MIT, and no official endorsement should be inferred.

Notes and references

[a] Department of Mechanical Engineering, City College of New York, New York, NY 10031, United States
[b] Department of Electrical and Computer Engineering, International Islamic University Malaysia, Jalan Gombak, Kuala Lumpur, Malaysia.
[c] Department of Mechanical Engineering, New York Institute of Technology, Old Westbury, New York 11568, United States.

1 C. J. Vörösmarty, P. McIntyre, M. O. Gessner, D. Dudgeon, A. Prusevich, P. Green, S. Glidden, S. E. Bunn, C. A. Sullivan and C. R. Liermann, *Nature,* 2010, **467**, 555-561.

2 P. R. Hunter, D. Zmirou-Navier and P. Hartemann, *Sci. Total Environ.,* 2009, **407**, 2621-2624.

3 A. D. Beaton, C. L. Cardwell, R. S. Thomas, V. J. Sieben, F. Legiret, E. M. Waugh, P. J. Statham, M. C. Mowlem and H. Morgan, *Environ. Sci. Technol.,* 2012, **46**, 9548-9556.

4 X. Qu, J. Brame, Q. Li and P. J. Alvarez, *Acc. Chem. Res.,* 2012, **46**, 834-843.

5 S. E. Hrudy and S. Rizak, *Journal-American Water Works Association,* 2004, **96**, 110-113.

6 T. M. Curtis, M. W. Widder, L. M. Brennan, S. J. Schwager, W. H. van der Schalie, J. Fey and N. Salazar, *Lab on a Chip,* 2009, **9**, 2176-2183.

7 L. M. Brennan, M. W. Widder, L. E. Lee and W. H. van der Schalie, *Toxicology in Vitro,* 2012, **26**, 736-745.

8 B. Wang, F. Wang, H. Jiao, X. Yang and C. Yu, *Analyst,* 2010, **135**, 1986-1991.

9 Y. Ding and R. Mutharasan, *Environ. Sci. Technol.,* 2010, **45**, 1490-1496.

10. U. Bohrn, A. Mucha, C. F. Werner, B. Trattner, M. Bäcker, C. Krumbe, M. Schienle, E. Stütz, D. Schmitt-Landsiedel, M. Fleischer, P. Wagner, M. J. Schöning, *Sensors Actuators B: Chem.*, 2013, vol. 182, pp. 58-65.

11 van der Schalie, William H, R. R. James and T. P. Gargan II, *Biosensors and Bioelectronics,* 2006, **22**, 18-27.

12 P. Banerjee and A. K. Bhunia, *Trends Biotechnol.,* 2009, **27**, 179-188.

13 C. Ziegler, *Fresenius J. Anal. Chem.,* 2000, **366**, 552-559.

14 A. K. Bhunia, P. Banada, P. Banerjee, A. Valadez and E. D. Hirleman, *Journal of Rapid Methods \& Automation in Microbiology,* 2007, **15**, 121-145.

15 D. A. Stenger, G. W. Gross, E. W. Keefer, K. M. Shaffer, J. D. Andreadis, W. Ma and J. J. Pancrazio, *Trends Biotechnol.,* 2001, **19**, 304-309.

16 G. T. Kovacs, *Proc IEEE,* 2003, **91**, 915-929.

17 J. Pancrazio, J. Whelan, D. Borkholder, W. Ma and D. Stenger, *Ann. Biomed. Eng.,* 1999, **27**, 697-711.

18 C. Lo, C. R. Keese and I. Giaever, *Exp. Cell Res.,* 1993, **204**, 102-109.

19 C. R. Keese and I. Giaever, *Engineering in Medicine and Biology Magazine, IEEE,* 1994, **13**, 402-408.

20 H. E. Ayliffe, A. B. Frazier and R. Rabbitt, *Microelectromechanical Systems, Journal of,* 1999, **8**, 50-57.

21 A. Han, L. Yang and A. B. Frazier, *Clinical cancer research,* 2007, **13**, 139-143.

22 C. Xiao and J. H. Luong, *Toxicol. Appl. Pharmacol.,* 2005, **206**, 102-112.

23 S. Arndt, J. Seebach, K. Psathaki, H. Galla and J. Wegener, *Biosensors and Bioelectronics,* 2004, **19**, 583-594.

24 X. Huang, D. Greve, D. Nguyen and M. Domach, 2003, **1**, 304-309.

25 R. Go, R. Bashir, A. Sarikaya, M. Ladisch, J. Sturgis, J. Robinson, T. Geng, A. Bhunia, H. Apple and S. Wereley, *Biomed. Microdevices,* 2001, **3**, 201-209.

26 J. F. Alder and J. J. McCallum, *Analyst,* 1983, **108**, 1169-1189.

27 K. A. Marx, *Biomacromolecules,* 2003, **4**, 1099-1120.

28 B. Wyszynski and T. Nakamoto, *IEEJ Transactions on Electrical and Electronic Engineering,* 2009, **4**, 334-338.

29 F. Li, J. H. Wang and Q. Wang, *Biosensors and Bioelectronics,* 2007, **23**, 42-50.

30 M. Pax, J. Rieger, R. H. Eibl, C. Thielemann and D. Johannsmann, *Analyst,* 2005, **130**, 1474-1477.

31 R. Lucklum and P. Hauptmann, *Measurement Science and Technology,* 2003, **14**, 1854.

32 S. Hong, E. Ergezen, R. Lec and K. A. Barbee, *Biomaterials,* 2006, **27**, 5813-5820.

33 Y. Qiu, R. Liao and X. Zhang, *Anal. Chem.,* 2008, **80**, 990-996.

34 F. Liu, F. Li, A. N. Nordin and I. Voiculescu, *Sensors,* 2013, **13**, 3039-3055.

35 I. Voiculescu, F. Li, F. Liu, X. Zhang, L. M. Cancel, J. M. Tarbell and A. Khademhosseini, *Sensors Actuators B: Chem.,* 2013, .

36 M. Schneider, I. W. Marison and U. von Stockar, *J. Biotechnol.,* 1996, **46**, 161-185.

37 F. Mégraud, V. Neman-Simha and D. Brügmann, *Infect. Immun.,* 1992, **60**, 1858-1863.

38 K. Martinelle and L. Häggström, *J. Biotechnol.,* 1993, **30**, 339-350.

39 T. Hassell, S. Gleave and M. Butler, *Appl. Biochem. Biotechnol.,* 1991, **30**, 29-41.

40 O. Braissant, *Mol. Genet. Metab.,* 2010, **100**, S53-S58.

41 S. S. Hecht, in *in Chemical Carcinogenesis,* ed. nonymous Springer, 2011, pp.53-74.

42 H. P. S. Wong, L. Yu, E. K. Y. Lam, E. K. K. Tai, W. K. K. Wu and C. Cho, *Toxicological Sciences,* 2007, **97**, 279-287.

43 J. F. Risher, F. L. Mink and J. F. Stara, *Environ. Health Perspect.,* 1987, **72**, 267.

44 M. Fiore, H. Anderson, R. Hong, R. Golubjatnikov, J. Seiser, D. Nordstrom, L. Hanrahan and D. Belluck, *Environ. Res.,* 1986, **41**, 633-645.

45 L. R. Goldman, M. Beller, H. Oregon and R. J. Jackson, *Archives of Environmental Health: An International Journal,* 1990, **45**, 141-147.

46 C. G. Marxer, M. C. Coen, T. Greber, U. F. Greber and L. Schlapbach, *Analytical and bioanalytical chemistry,* 2003, **377**, 578-586.

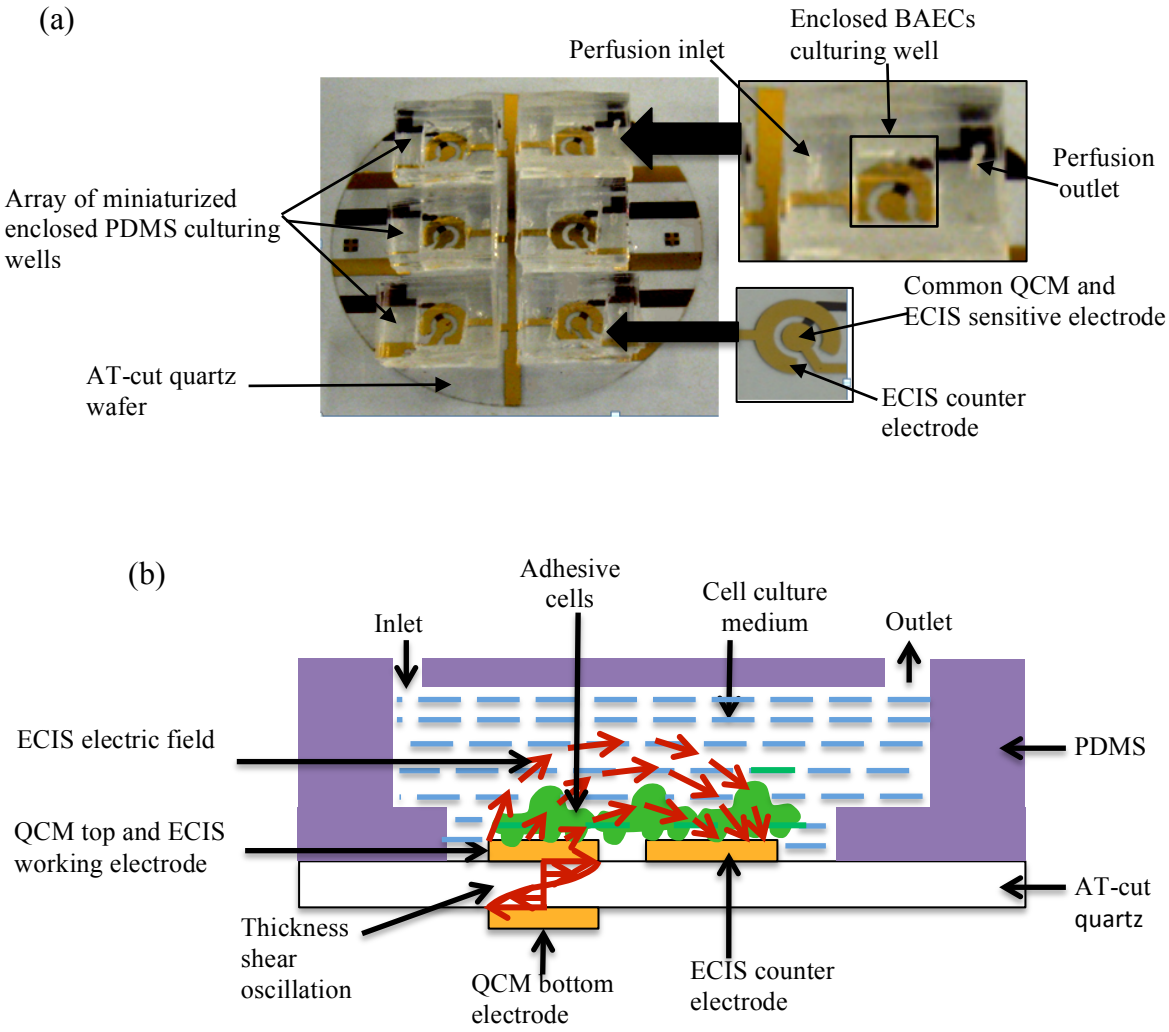

Figure 1 (a): Multiparametric sensor array integrated with miniaturized enclosed polymeric culturing chambers. (b) Cross-section of the multiparametric sensor and fluidic biochip. The working and bottom electrodes have a diameter of 2 mm. Two layer PDMS chambers (8mm×8mm×3mm) enclose the electrodes and were bonded on sensor surface using silicone glue. The whole quartz wafer containing 6 multiparametric sensors has a diameter of 5 cm.

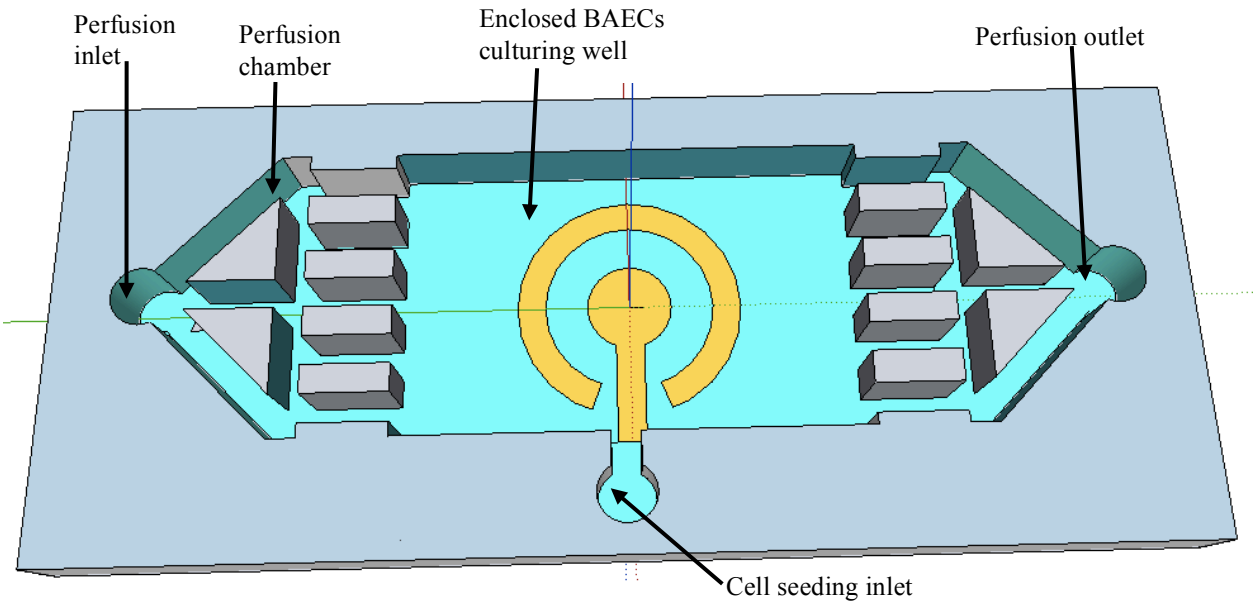

Figure 2. Top view of microfluidic biochip with perfusion chambers, inlet, outlet and cell seeding inlet.

(a)

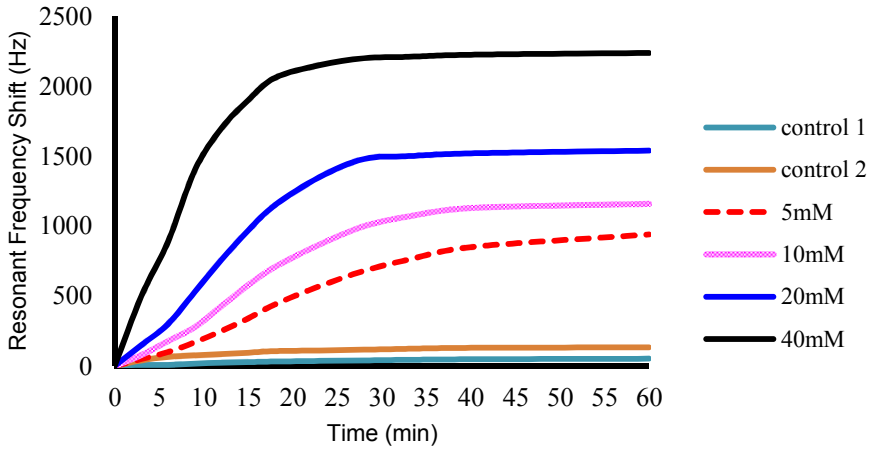

(b)

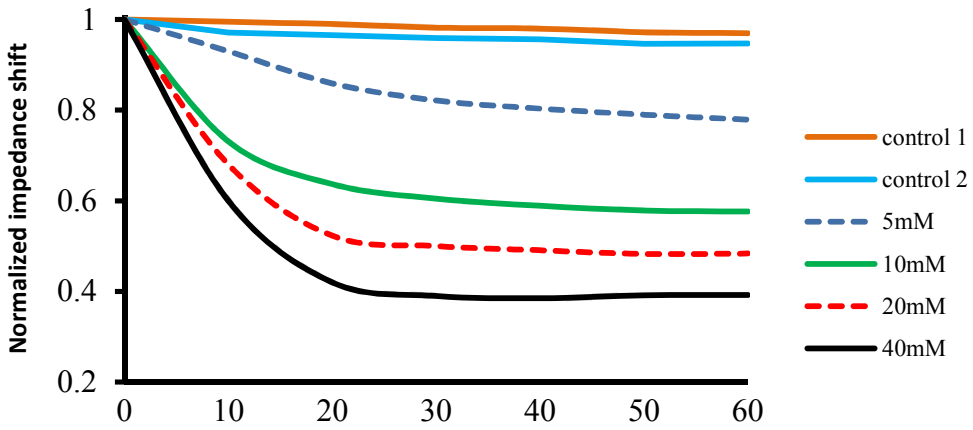

(c)

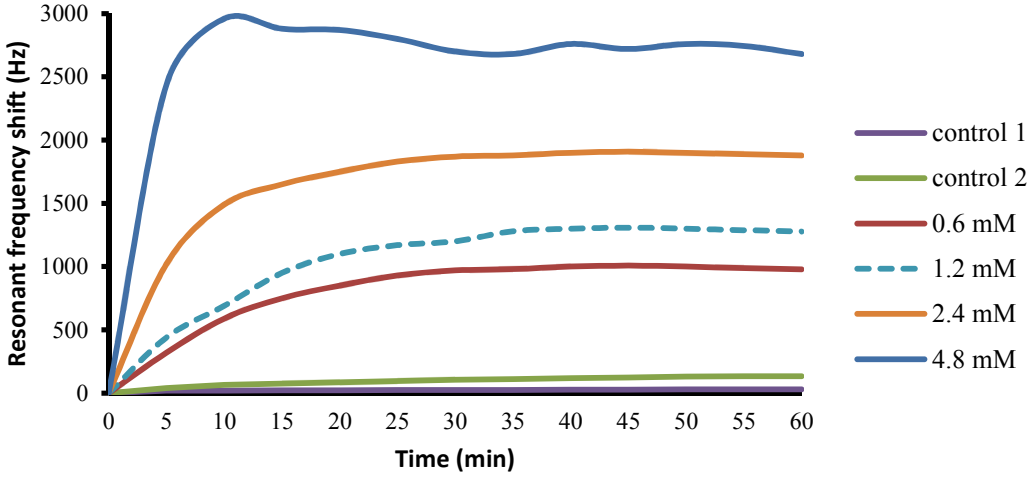

(d)

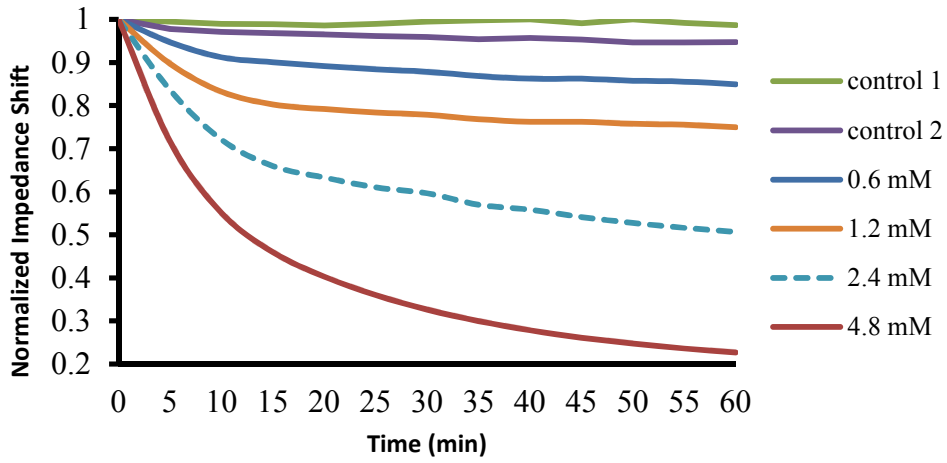

(e)

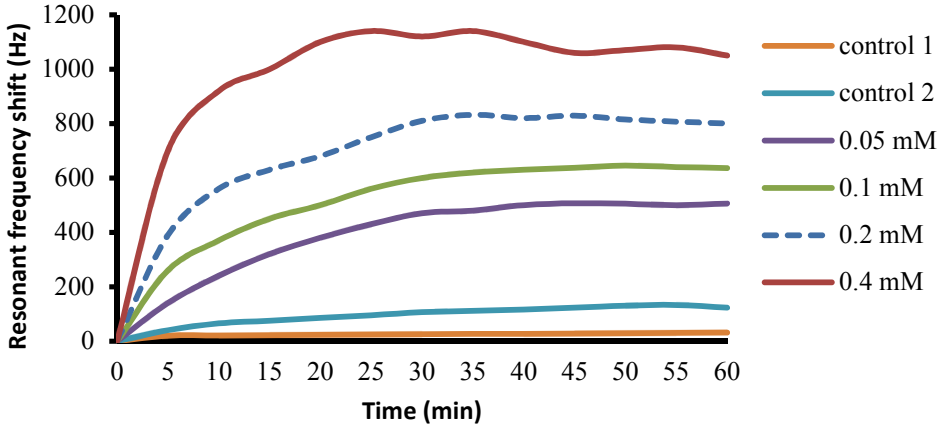

(f)

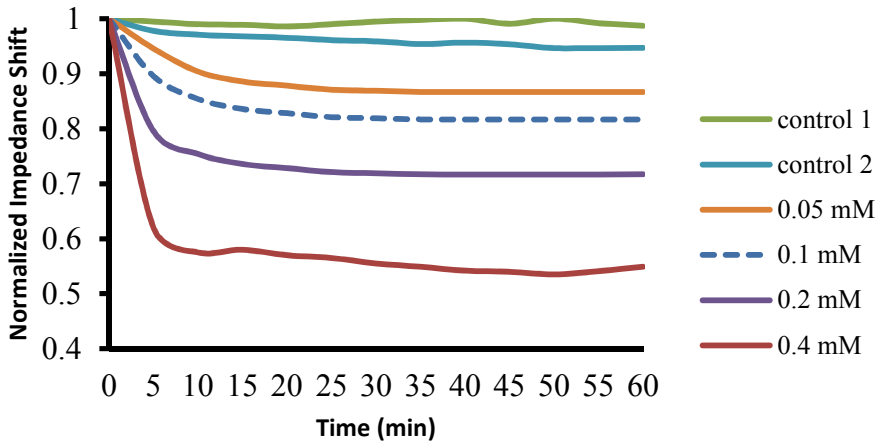

Figure 3: Toxicity testing of ammonia in DI water. Simultaneous measurements of (a) resonant frequency and (b) impedance were performed for 5 mM, 10 mM, 20 mM and 40 mM of ammonia. Results in control 1 (cells with media) and control 2 (cells with DI water) show stable signal and minor shifts respectively. Responses of BAECs to 0.6 mM, 1.2 mM, 2.4 mM and 4.8 mM of nicotine were monitored simultaneously with (c) resonant frequency measurement and (d) impedance measurement. Control 1 and control 2 correspond to the experiment of cells with media and cells with DI water, respectively. Simultaneous measurements of (e) resonant frequency and (f) impedance with different concentrations of aldicarb at 0.05 mM, 0.1 mM, 0.2 mM and 0.4 mM. The confluent monolayer of BAEC responses to aldicarb was monitored for one hour. In control 1, cells are cultured in normal culture media and in control 2 cells are maintained in DI water.

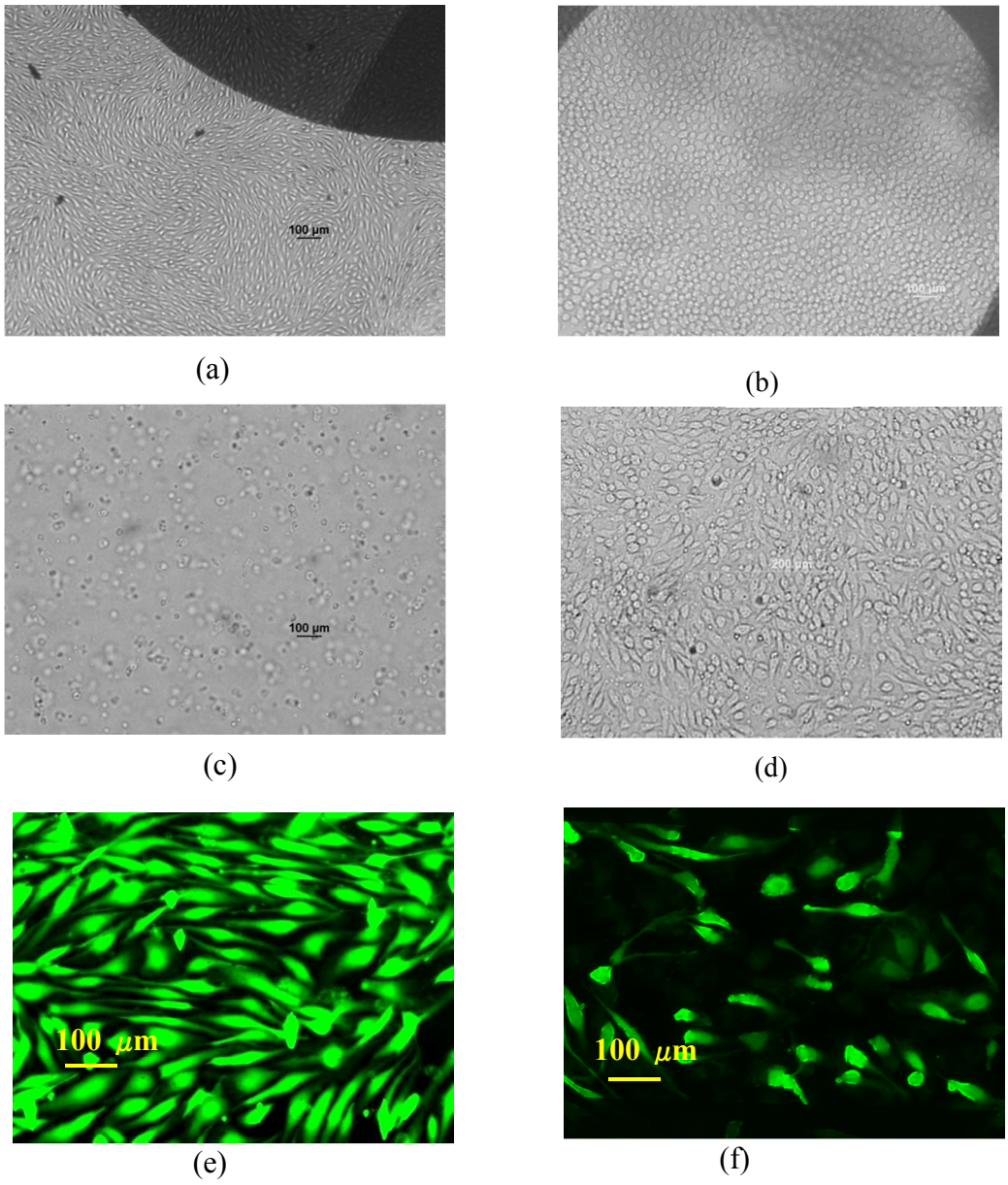

Figure 4. Microscope images of BAECs with seeding density of 1×10^5 cells/cm^2 cultured on the multiparametric device; (a) BAECs' uniform monolayer on the sensor before exposure to toxicant, after 45 hours in culture. (b) BAECs 30 minutes after exposure to 0.1mM aldicarb, (c) BAECs 30 minutes after exposure to 40 mM ammonia (d) BAECs 30 minutes after exposure to 2.4 mM nicotine, (e) fluorescent microscope images of BAECs stained with Calcein AM after 45 hours in culture (d) fluorescent microscope images of BAECs 10 minutes after exposure to 20 mM ammonia. The BAECs used in these experiments were from passage 7 to passage 10. In Figures (e) and (f) live BAECs stained by Calcein AM emit green fluorescence after fluorescence light excitation. The color of apoptotic BAECs is black, because they cannot be stained with Calcein AM.

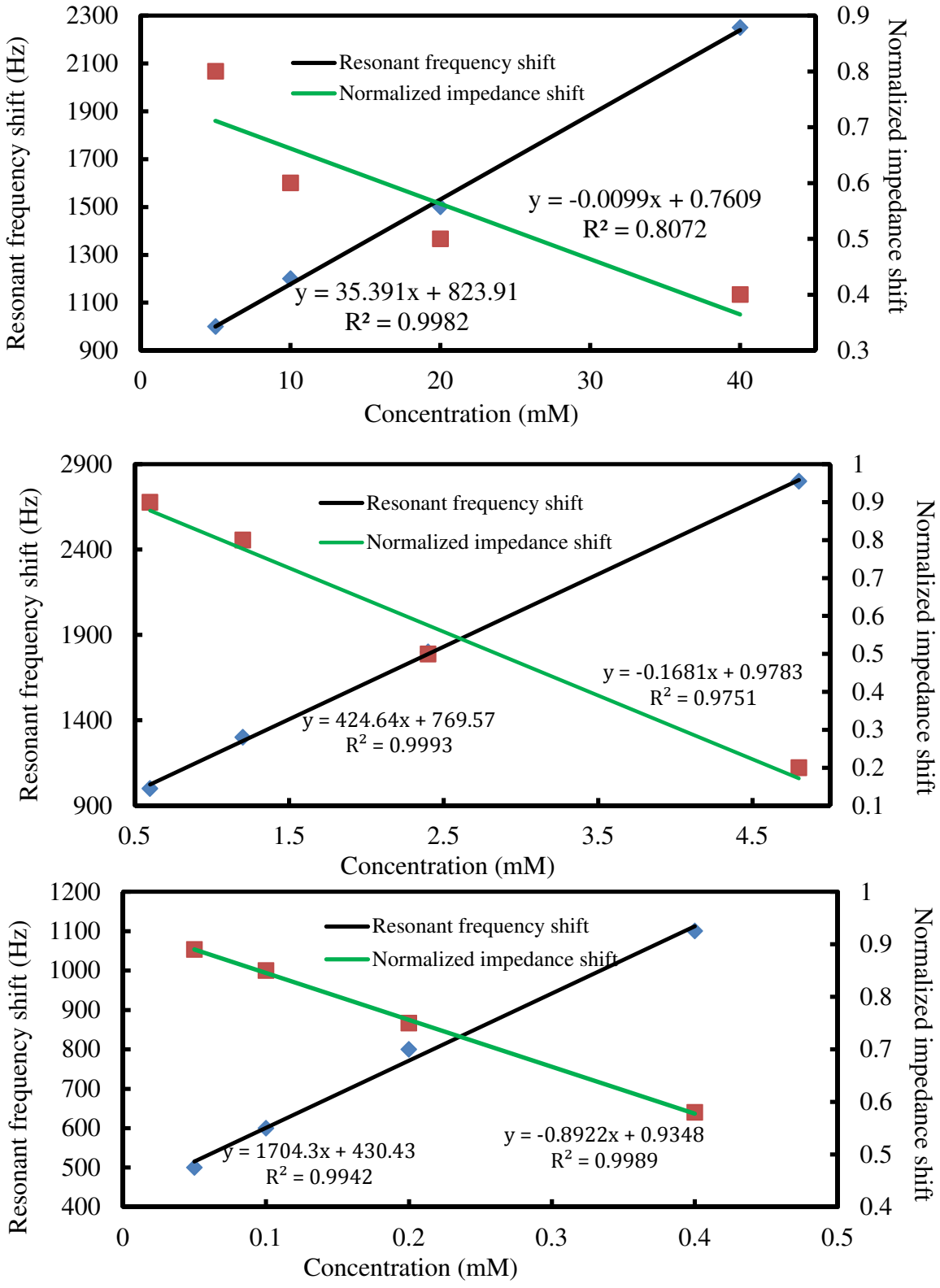

Figure 5: Characterization of the multiparametric sensor linearity between measurements and different chemical concentrations: (a) ammonia, (b) nicotine and (c) aldicarb.